PARAMAGNETIC NMR SPECTROSCOPY AS A TOOL FOR STUDYING THE ELECTRONIC STRUCTURES OF LANTHANIDE AND TRANSITION METAL COMPLEXES

Cite this: *INEOS OPEN*, **2019**, *2 (5)*, 153–162
DOI: 10.32931/io1922r

Received 8 October 2019,
Accepted 2 November 2019

http://ineosopen.org

A. A. Pavlov*

Nesmeyanov Institute of Organoelement Compounds, Russian Academy of Sciences, ul. Vavilova 28, Moscow, 119991 Russia

Abstract

Nuclear magnetic resonance (NMR) spectroscopy is traditionally used to study diamagnetic chemical compounds, whereas for paramagnetic compounds this method is often mistakenly perceived as unsuitable. Although the foundations of paramagnetic NMR spectroscopy were laid over 50 years ago, the application scope of this method is generally restricted to biological and medical studies, while in exploration of the properties of chemical compounds paramagnetic NMR did not gain widespread use.

The current review presents the examples of application of paramagnetic NMR spectroscopy for studying the electronic structures of lanthanide and transition metal complexes. The key features and problems are considered that should be taken into account while using NMR spectroscopy in practice both for investigation of the electronic structures and also for other purposes.

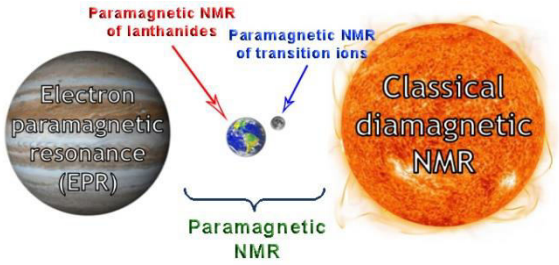

Key words: paramagnetic NMR, electronic structure, magnetic properties, lanthanides, transition metals.

1. Introduction

Recent years have witnessed a noticeable growth in the number of functional materials based on metal complexes that display unusual magnetic properties, such as spin switches [1], single-molecule magnets [2, 3], elements of quantum computers [4], and so on. The progress in these fields facilitates the development of new physical methods for investigation of magnetic properties and electronic structures of various chemical compounds (high-field and terahertz EPR spectroscopy, magnetic circular dichroism, *etc.*). In this respect, modern NMR spectroscopy seems to be underestimated: the annual number of publications on paramagnetic NMR does not exceed 50 and there is no significant growth in publication activity over the years [5]. A major part of the reports are devoted to the biological and medical applications: paramagnetic labels for investigation of the structures of biological macromolecules in solution [6–9], shift and relaxation agents [10–12], and *in vivo* temperature and pH sensors [10, 13, 14].

The goal of this review is to demonstrate the possibilities of paramagnetic NMR spectroscopy for investigation of the electronic structures of different lanthanide and transition metal complexes, which are of special interest as new magnetic functional materials. Particular attention will be drawn to the peculiarities and problems that arise during practical application of this method. The advantages and disadvantages as well as the application scope of this method will be compared to those of classical methods for investigation of magnetic properties (EPR spectroscopy and magnetometry).

2. Lanthanide complexes

An electronic structure of the ground state of a free lanthanide ion represents a set of degenerate $2J+1$ levels, where J is the quantum number of a total angular momentum. As a rule, the ligand field effects in metal coordination compounds are significantly weaker than the spin–orbit interaction, since atomic *f*-orbitals of the lanthanide ions are weakly involved in the formation of bonding molecular orbitals. Nevertheless, it is the crystal field that removes degeneration of $2J+1$ levels and, thus, determines the magnetic properties of a compound. The diverse magnetic properties of lanthanide complexes are extensively studied for the following current and potential applications: single-molecule magnets [2], paramagnetic probes [6–9], shift and relaxation agents [10–12], *in vivo* temperature and pH sensors in MRI [10, 13, 14], and elements of quantum computers [4]. Therefore, investigation of the ligand field parameters in lanthanide complexes is crucial for the mentioned application fields [15, 16].

A conventional method for elucidation of the electronic structures of lanthanide complexes is luminescence spectroscopy [17–19]. A fine structure of luminescence bands stems from the splitting under ligand crystal field effect and, consequently, can be used to define the electronic levels of the

ground state. However, in many cases, a signal in the luminescence spectrum is not resolved enough to reveal a fine structure, which makes this approach unsuitable for these systems.

NMR spectroscopy and magnetometry were used for the first time to determine the ligand field parameters in lanthanide complexes by the group of Prof. N. Ishikawa in 2003 [20]. Their work was concerned with anionic phthalocyanine complexes of lanthanides $\mathbf{LnPc_2^-}$ (Scheme 1), which appeared to be the first representatives of single-molecule magnets based on lanthanide complexes [21, 22]. To describe the observed effects, the authors used the Hamiltonian which expresses the ligand field parameters through the Stevens operators [23]:

$$\hat{\boldsymbol{H}}_{LF} = \sum_{q=0}^{2} B_2^q \hat{\boldsymbol{O}}_2^q + \sum_{q=0}^{4} B_4^q \hat{\boldsymbol{O}}_2^q + \sum_{q=0}^{6} B_6^q \hat{\boldsymbol{O}}_6^q \qquad (1)$$

where $\hat{\boldsymbol{O}}_2^q$ are the polynomial functions of total momentum operators $\hat{\boldsymbol{J}}_z$, $\hat{\boldsymbol{J}}_+$,$\hat{\boldsymbol{J}}_-$ listed in Ref. [24]. Different symmetries of the ligand crystal fields will be characterized by the different set of parameters; for example, in the case of $\mathbf{LnPc_2^-}$ complexes with D_{4d} symmetry, the Hamiltonian becomes essentially simpler:

$$\hat{\boldsymbol{H}}_{LF}^{D_{4d}} = B_2^0 \hat{\boldsymbol{O}}_2^0 + B_4^0 \hat{\boldsymbol{O}}_4^0 + B_6^0 \hat{\boldsymbol{O}}_6^0 \qquad (2)$$

Furthermore, the authors assume that all the field parameters depend linearly on the number of *f*-electrons (n) in the series of isostructural lanthanide complexes from f^8 (Tb^{3+}) to f^{13} (Yb^{3+}):

$$B_k^q(n) = a_k^q + b_k^q(n - n_0) \qquad (3)$$

where n_0 is the average number of *f*-electrons in the series of the ions under consideration. This assumption is not rigorously proved by the authors and is explained by the fact that, in the lanthanide series, the field parameters must change regularly depending on the number of *f*-electrons. However, this assumption is very important for the accuracy of definition of the field parameters, since it reduces the number of unknown parameters from 3N (N is the number of isostructural complexes under investigation) to 6, and allows one to solve the problem of overparametrization which was described in several reports [25, 26]. It should be noted that some authors question this assumption [27].

The approach consists in the multidimensional optimization of the crystal field parameters which describe the experimental data obtained by NMR spectroscopy and magnetometry best of all (Scheme 2). These two methods are parent for solution to this problem, since they allow one to determine experimentally some components of the magnetic susceptibility tensor $\boldsymbol{\chi}$. Whereas powder magnetometry affords isotropic value of $\overline{\boldsymbol{\chi}}$, the NMR spectra provide the information about anisotropy of this tensor $\Delta\chi_{ax}$, $\Delta\chi_{rh}$:

$$\overline{\boldsymbol{\chi}} = \frac{\chi_{zz}+\chi_{yy}+\chi_{xx}}{3} \qquad (4a)$$

$$\Delta\chi_{ax} = \chi_{zz} - \frac{\chi_{yy}+\chi_{xx}}{2} \qquad (4b)$$

$$\Delta\chi_{rh} = \chi_{yy} - \chi_{xx} \qquad (4c)$$

Generally, a chemical shift of the nucleus of a paramagnetic compound in the NMR spectrum can be divided into three contributions: diamagnetic, contact, and pseudocontact (5).

$$\delta_{obs} = \delta_{dia} + \delta_{cs} + \delta_{pcs} \qquad (5)$$

The diamagnetic contribution arises due to the shielding of nuclei by electron clouds, *i.e.*, it can be considered as a classical chemical shift of a diamagnetic compound. The other two contributions have paramagnetic nature, *i.e.*, they appear upon interaction of magnetic moments of an unpaired electron with a nucleus (hyperfine interaction). The contact shift results from delocalization of the unpaired electron from the paramagnetic metal ion to the nucleus through a system of molecular orbitals and, thus, is proportional to the spin density (the electron density of the unpaired electron) at the nucleus location (ρ):

$$\delta_{cs} = \frac{\mu_0 \mu_B^2 g_e^2 (S+1)}{9kT} \cdot \rho \qquad (6)$$

where S is the electron spin, μ_B is the Bohr magneton.

It should be noted that relation (6) is valid in the case of several assumptions; this problem was discussed in detail in a recent review [28].

The pseudocontact (dipole) shift arises due to the dipole–dipole interaction of magnetic moments of the unpaired electron and the nucleus:

$$\delta_{pcs} = \frac{1}{12\pi r^3}\left[\Delta\chi_{ax}(3cos^2\theta - 1) + \frac{3}{2}\Delta\chi_{rh}sin^2\theta cos2\varphi\right] \qquad (7)$$

where r, θ, φ are the spherical coordinates of the nucleus in the eigensystem of coordinates of tensor $\boldsymbol{\chi}$. Hence, knowing the value of the pseudocontact shift and the coordinates of nuclei from the molecule structure, it is easy to calculate the values of anisotropy parameters of tensor $(\Delta\chi_{ax}, \chi_{rh})$.

It should be noted that the authors neglected the effect of the contact shift for complexes $\mathbf{LnPc_2^-}$ as well as for all phthalocyanine and porphyrin complexes considered in this review below.

Indeed, due to the weak contribution of *f*-electrons to the metal–ligand bonds (compared, for example, to *d*-electrons of transition metal ions), there is no significant delocalization of the spin density on the ligand nuclei [29]. However, it was shown that for some lanthanide complexes (including phthalocyanine derivatives [30]) the contact contribution to the chemical shift can be essential [31]. Hence, in the author's opinion, the problem of consideration of the contact contribution for lanthanide complexes is still controversial.

The components of tensor $\boldsymbol{\chi}$ (χ_{zz}, χ_{yy}, and χ_{xx}) are connected with the energy levels and, consequently, with the Hamiltonian (1) parameters through the Van Vleck equations [32]. The optimization of the crystal field parameters was carried out until the best convergence of the experimental and calculated values of $\overline{\boldsymbol{\chi}}$ (magnetometric data) and $\Delta\chi_{ax}$ (NMR data). A total algorithm of the optimization process is presented in Scheme 2.

It is important to note that Ishikawa [25] showed that the application of the data of only one of two methods also leads to the problem of overparametrization, *i.e.*, the experimental data can be described rather good by a broad set of parameters, which makes impossible the accurate definition of the energies of electronic levels. In particular, the application of only one of

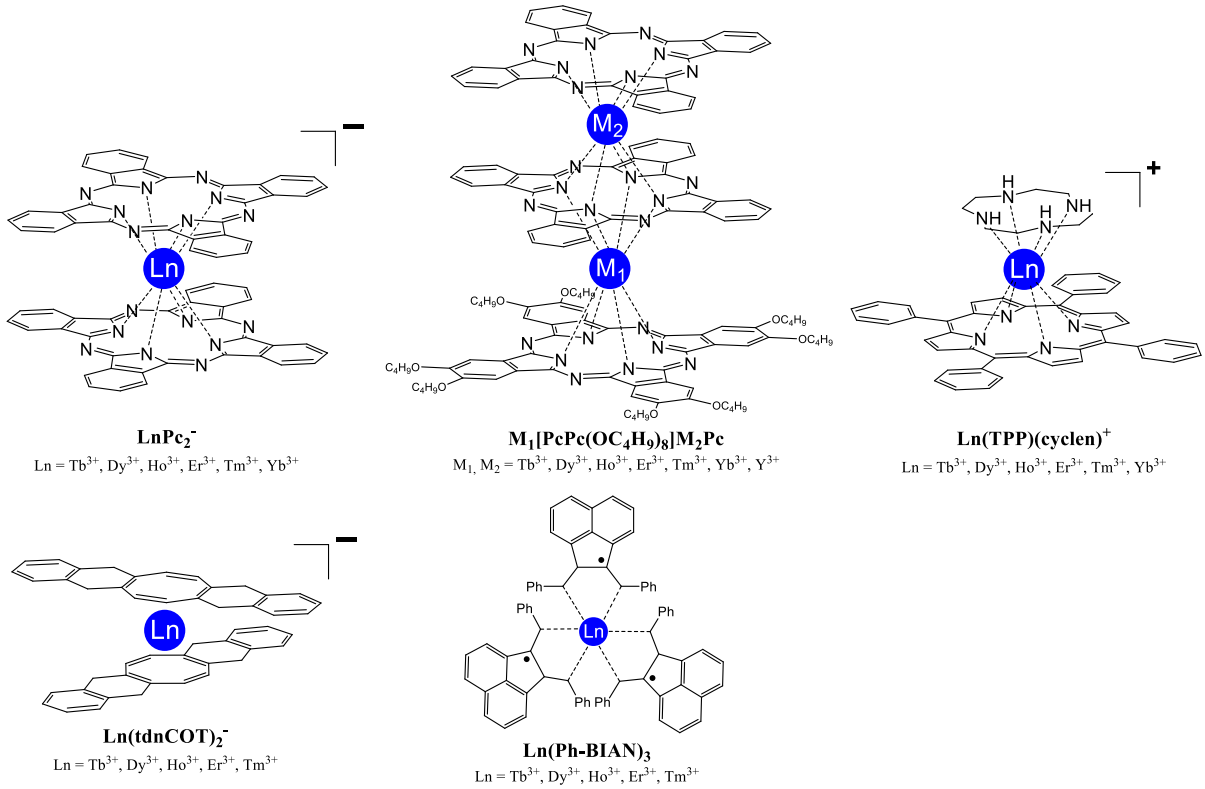

Scheme 1. Lanthanide complexes considered in the review.

these methods leads to the errors in the definition of parameters a_2^0, a_4^0, and a_6^0 (see equation (3)) approximately equal to 60, 25, and 22% (according to the magnetometry data) and 5, 10, and 20% (according to the NMR data), respectively. Only in the case of simultaneous modeling of the data of two methods, the dispersions of a_2^0, a_4^0 and a_6^0 drop (the corresponding errors composed about 1, 2, and 3%), which testifies reliability of this result. In turn, the latter evidences the importance of the NMR data in exploration of the electronic structures of lanthanide complexes.

The resulting values of the ligand field parameters allowed for the definition of the energies of ground-state electronic levels [20] (Fig. 1). Among the compounds explored, only for

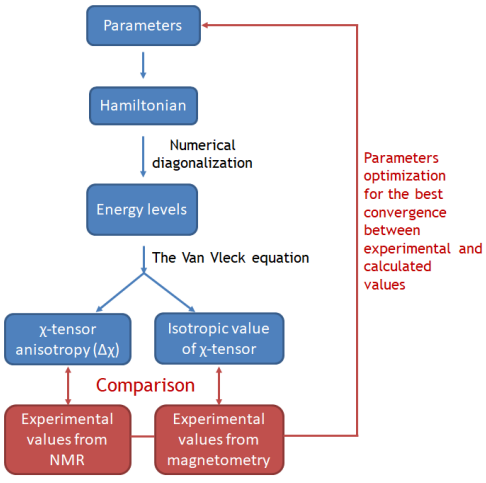

Scheme 2. Algorithm for optimization of the ligand crystal field parameters based on the data of NMR spectroscopy and magnetometry.

complex **TbPc$_2^-$** the lowest Kramers doublet (KD) corresponds to the highest value m_J = ±6, which indicates an essential magnetic anisotropy along C_4 symmetry axis. The energy of the second KD composes 436 cm^{-1}, which is much higher than kT even at room temperature, *i.e.*, the properties of complex **TbPc$_2^-$** are almost completely defined by the lowest KD. This result is in good agreement with the efficiency of lanthanide phthalocyanine complexes as single-molecule magnets (SMM). Since the magnetic anisotropy and the high energy of KD leads to an essential magnetization reversal barrier, it should be expected that just Tb^{3+} ions will exhibit the best SMM properties. Indeed, for diamagnetically diluted complexes **LnPc$_2^-$** doped with Y^{3+}, the effective magnetization reversal barriers for Tb^{3+} complexes are much higher than those for analogous Dy^{3+} complexes (U_{Dy} = 28 cm^{-1}, U_{Tb} = 230 cm^{-1} (x_Y = 25%) [21], U_{Dy} = 31 cm^{-1}, U_{Tb} = 260 cm^{-1} (x_Y = 2%) [33]). An analogous situation was observed for trinuclear complexes [34, 35] as well as for other phthalocyanine complexes [36].

In the case of heterobimetallic complexes **Ln[PcPc(OC$_4$H$_9$)$_8$]YPc** and **Y[PcPc(OC$_4$H$_9$)$_8$]LnPc** (Scheme 1), the presence of the yttrium ion reduces the complex symmetry compared to **LnPc$_2^-$** to C_4 group. As a result, the Hamiltonian (1) includes additional terms (q = 4) [24]:

$$\hat{H}_{LF}^{C_4} = B_2^0\hat{O}_2^0 + B_4^0\hat{O}_4^0 + B_4^4\hat{O}_4^4 + B_6^0\hat{O}_6^0 + B_6^4\hat{O}_6^4 \qquad (8)$$

The application of an analogous approach to the analysis of the NMR spectroscopic and magnetometric data afforded unambiguous values of the crystal field parameters for complexes **Ln[PcPc(OC$_4$H$_9$)$_8$]YPc** [37] and **Y[PcPc(OC$_4$H$_9$)$_8$]LnPc** [38]. The values of terms B_4^4 and B_6^4 in the crystal field Hamiltonian (8) appeared to be nonzero, which

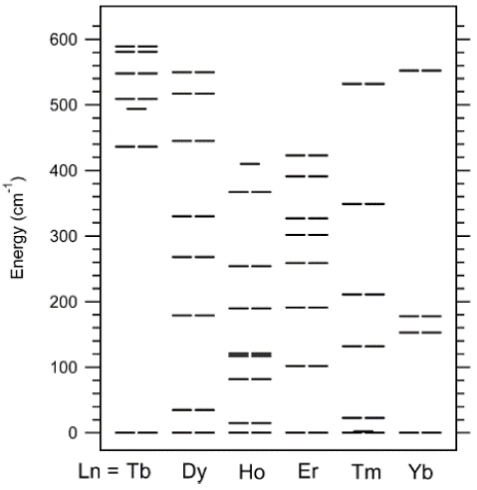

Figure 1. Electronic structure of the ground state of complexes **LnPc²⁻**. (Reprinted with permission from N. Ishikawa *et al.*, *Inorg. Chem.*, **2003**, *42*, 2440–2446. DOI: 10.1021/ic026295u. Copyright (2003) American Chemical Society)

leads to certain consequences for the electronic structures of the complexes: the electronic levels do not correspond to neat states m_J and represent a combination of different states m_J, which affords additional routes for magnetization relaxation if these complexes are used as SMM [39].

Based on the data about the electronic structures of complexes **Ln[PcPc(OC$_4$H$_9$)$_8$]YPc** and **Y[PcPc(OC$_4$H$_9$)$_8$]LnPc**, the bimetallic homonuclear complexes of a general formula **Ln[PcPc(OC$_4$H$_9$)$_8$]LnPc** bearing two paramagnetic metal ions were studied (Scheme 1) [38]. Upon description of these complexes, among other issues, one should take into account the electron–electron interaction between two paramagnetic Ln^{3+} ions, which includes the dipole and exchange interactions:

$$\hat{\boldsymbol{H}} = \hat{\boldsymbol{H}}_{LF}^{M_1} + \hat{\boldsymbol{H}}_{LF}^{M_2} + \hat{\boldsymbol{V}}_{M_1M_2}^{dip} + J_{ex}(\hat{\boldsymbol{J}}_1 \cdot \hat{\boldsymbol{J}}_2) \qquad (9)$$

Since the ligand field parameters for the heteronuclear complexes were determined earlier and the dipole interaction depends on mutual disposition of the lanthanide ions, which is known from the complex structure, the first three terms in relation (9) are known; as for the exchange interaction (the fourth term), Ishikawa *et al.* [38] assumed that it is negligibly small. A good agreement between the calculated values of χT and the experimental data confirmed this assumption and allowed for the first detailed study of the *f–f* electronic interaction in lanthanide complexes.

Lanthanide complexes of porphyrins, featuring similar symmetries, are also of certain interest as promising SMMs [40, 41]. However, NMR spectroscopic studies of a series of cationic complexes **Ln(TPP)(cyclen)$^+$** (Scheme 1) showed that the electronic structures of these compounds significantly differ from those of the phthalocyanine analogs [42]. In particular, the energy of the second KD of **Tb(TPP)(cyclen)$^+$** is considerably lower (*cf.* 150 cm^{-1} with 436 см$^{-1}$ for complex **TbPc$_2^-$**), and, in the case of complex **Dy(TPP)(cyclen)$^+$**, the lower KD complies with m_J = ±11/2 in contrast to the phthalocyanine analogs for which m_J = ±13/2. The lower value of the second KD energy and the lower value of $|m_J|$ of the lower KD indicate the lower magnetic anisotropy and, consequently, the inferior SMM properties. Indeed, the comparison of analogous complexes bearing phthalocyanine and porphyrin ligands shows that the magnetization reversal barriers of the latter are lower [43].

Although phthalocyanine and porphyrin complexes of lanthanides display a relative conformational rigidity, the large lanthanide radius and, as a consequence, the large space in the coordination sphere often favor conformational lability of the ligands. Thus, investigation of the structures of lanthanide complexes in solution is often associated with the problem of interpretation of the data due to active conformational dynamics and different structural changes [44, 45]. It should be noted that this problem is especially important for paramagnetic compounds, since the value of their shifts strongly depend on the nucleus coordinates (see (7)). This can be illustrated by double-decker complexes derived from substituted tetraoctatetraenide ligands which have saturated conformationally labile hydrocarbon moieties. Based on the analysis of paramagnetic NMR spectra, Hiller *et al.* [46] showed that complexes **[Ln(tdnCOT)$_2$]$^-$** (Scheme 1) exist in solution in the form of two conformers, in which ligand **tdnCOT** is spatially bent outward (an exo conformer) or inward (an endo conformer) relative to the other ligand in the complex. Consideration of both of the conformations (54% of the exo conformer at room temperature) allowed the authors to reliably define the values of $\Delta\chi_{ax}$, which are required for investigation of the electronic structure. Furthermore, in this report, the authors, unlike their earlier studies [20, 25, 37, 38], also took into account a contact contribution to the chemical shift. Indeed, it was shown that this contribution is essential for the related complexes [31]. Hence, the following equation was used to define the total value of a chemical shift:

$$\delta_{obs}^{i,j} = \delta_{orb}^{i,j} + \delta_{CS}^{i,j} + \delta_{PCS}^{i,j} = \delta_{Y^{3+}}^{i} + \frac{\mu_B}{3kT\gamma^i}\frac{A^i}{\hbar}\langle S_z\rangle^j + \frac{1}{12\pi}G^i\Delta\chi_{ax}^j \qquad (10)$$

where indices *i* and *j* refer to the nucleus, for which the NMR signal is observed, and to the lanthanide ion, respectively; $\delta_{Y^{3+}}^{i}$ is the chemical shift of the nucleus *i* in an analogous yttrium(III) diamagnetic complex; A^i is the constant of hyperfine interaction of the nucleus *i*. This assumption is based on the isostructural natures of the complexes under consideration [47, 48]. Furthermore, the geometric factors of the nuclei G^i are taken to be the same for the complexes of all lanthanide ions. The values of $\langle S_z\rangle^j$ for each ion were taken from the literature [49, 50]. It should be mentioned that the cases are possible when the values of $\langle S_z\rangle^j$ strongly differ from the reported data [51]; therefore, this assumption should be carefully taken into account during the analysis of the NMR data for lanthanide complexes.

On the other hand, the authors used an elegant alternative route for the definition of $\Delta\chi_{ax}$ and, thus, indirectly confirmed the legitimacy of their assumptions. This approach consists in the analysis of ^{2}H NMR spectra of the deuterated analogs, in which the signals split due to the residual quadrupole interaction (RDC) of the deuterium nuclei. The value of RDC is directly connected with the value of anisotropy $\Delta\chi_{ax}$ [31, 48, 52]:

$$\left|\Delta\nu_Q\right| = \left|\frac{(e^2qQ/h)B_0^2}{20\mu_0 kT}(3cos^2\theta - 1)\Delta\chi_{ax}\right| \qquad (11)$$

where $\Delta\nu_Q$ is the observed signal splitting, Hz; Q is the constant of quadrupole interaction, Hz.

The values of $\Delta\chi_{ax}$ obtained by two independent methods appeared to be almost the same within the measurement accuracies, which evidences their reliability. The resulting values were used to define the ligand field parameters, but the magnetometric data were not included in the analysis [46]. Although Ishikawa [25] stated the problem of overparametrization upon application of the NMR data without magnetometric ones, this is not discussed in Ref. [46].

The resulting energies of electronic levels of the ground states for complexes **[Ln(tdnCOT)$_2$]$^-$** (Fig. 2) showed that the highest magnetic anisotropy is exhibited by Er^{3+} and Tm^{3+} derivatives, which feature the maximum values of $|m_J|$ of the lower KD (±15/2 and ±6, respectively). The results are in good agreement with the levels calculated earlier by the CASSCF method [53, 54]. This result is out of the common concepts stating that the most anisotropic ions are Tb^{3+} and Dy^{3+} [55]. Indeed, significant magnetic anisotropies of Er^{3+} and Tm^{3+} complexes are confirmed by their SMM behavior [56]: a magnetization reversal barrier for **Er[COT]$_2^-$** composed 286 K, whereas for **Dy[COT]$_2^-$** it was only 11 K [54]. In particular, it was shown that for **Dy[COT]$_2^-$** the probability of a transition between the levels of the lower KD is higher by six orders of magnitude than that for **Er[COT]$_2^-$** [54]; for **Dy[COT]$_2^-$** this transition is the main route for magnetization relaxation. The most efficient process of relaxation for **Er[COT]$_2^-$** affects the levels of the second and third KD (m_J = ± 13/2 and ± 1/2) with the energy of 175 and 194 cm^{-1}, respectively, which is in good agreement with the experimental magnetization reversal barrier of 199 cm^{-1}.

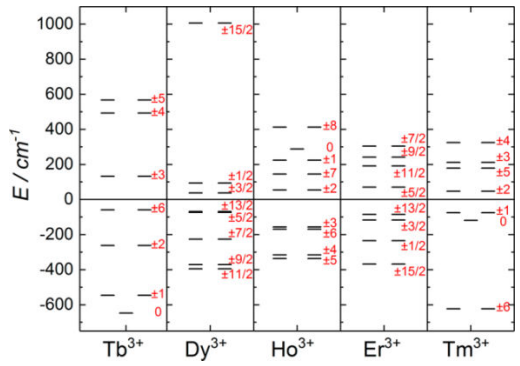

Figure 2. Energy levels of the ground state of **[Ln(tdnCOT)$_2$]$^-$**. (Reprinted with permission from M. Hiller *et al.*, *Inorg. Chem.*, **2017**, *56*, 15285–15294. DOI: 10.1021/acs.inorgchem.7b02704. Copyright (2017) American Chemical Society)

Another interesting class from the viewpoint of paramagnetic NMR includes the complexes formed by radicals as ligands. As a rule, the NMR spectra of organic radicals are poorly resolved due to a rapid nuclear relaxation, which renders EPR spectroscopy more suitable for their investigation. However, the complexes formed by these ligands and paramagnetic metal ions feature essentially slower nuclear relaxation, which makes NMR spectroscopy applicable for their exploration. Hence, the radical nature of the ligand does not hamper the application of NMR spectroscopy for elucidation of the electronic structures of metal complexes and even enables its use for investigation of these radicals themselves, which is impossible for their free forms.

A general relation for the observed chemical shift of the nucleus i ($\delta_{obs}^{i,j}$) must take into account the effect of both the paramagnetic lanthanide ion j and the unpaired ligand electron:

$$\delta_{obs}^{i,j} = \delta_{orb}^{i} + \delta_{RC}^{i} + \delta_{RPC}^{i} + \delta_{MC}^{i,j} + \delta_{MPC}^{i,j} \qquad (12)$$

where indices *RC* and *RPC* refer to the contact and pseudocontact shifts induced by the radical, respectively; indices *MC* and *MPC* correspond to the analogous shifts induced by the paramagnetic ion.

As a rule, the unpaired electron of the radical is strongly delocalized along the whole ligand molecule; as a result, the analysis of chemical shifts is very complicated, since it requires the knowledge of the spin-density distribution in the molecule. A simple method to overcome these difficulties is to use an isostructural complex with the diamagnetic metal ion (La^{3+}, Lu^{3+}, Y^{3+}), which shifts contain the shifts induced by the radical unpaired electron:

$$\delta_{obs}^{i,Y^{3+}} = \delta_{orb}^{i} + \delta_{RC}^{i} + \delta_{RPC}^{i} \qquad (13)$$

Hence, expression (12) becomes considerably simpler and leads to relation (10):

$$\delta_{obs}^{i,j} = \delta_{obs}^{i,Y^{3+}} + \delta_{MC}^{i,j} + \delta_{MPC}^{i,j} = \delta_{obs}^{i,Y^{3+}} + \frac{\mu_B}{3kT\gamma^i}\frac{A^i}{\hbar}\langle S_z\rangle^j + + \frac{1}{12\pi}G^i\Delta\chi_{ax}^j \qquad (14)$$

However, it is necessary to make several remarks, which stem from this assumption. First of all, this approach is applicable only in the case of isostructural complexes, in which the distributions of the unpaired electron of the radical are the same. Secondly, the observation of signals of the radical complex with the diamagnetic metal ion can be complicated due to a rapid nuclear relaxation.

Nevertheless, Hiller *et al.* [57] successfully used this approach for radical complexes **Ln(Ph-BIAN)$_3$** (Scheme 1). The values of $\Delta\chi_{ax}$ for these compounds were defined using equation (14). The authors also indicate that the radical nature of ligands can strengthen the delocalization of the unpaired *f*-electron and, consequently, can lead to significant contact shifts, which were estimated using DFT calculations (B3LYP and TPSSh functionals). An independent assessment of the values of $\Delta\chi_{ax}$ according to RDC with ^{2}H nuclei led to the same results within the measurement accuracy. Furthermore, the resulting values of $\Delta\chi_{ax}$ are in good agreement with the theoretical predictions [58].

Hence, NMR spectroscopy in its paramagnetic version can be successfully used for investigation of diverse lanthanide complexes: anionic, cationic, and neutral; mono- and bimetallic; the complexes bearing organic radicals. NMR spectroscopy allows one to study the structures in solution, which can differ from the crystalline ones due to conformational dynamics. One of the key features of NMR is the opportunity to study the structures of complexes and, consequently, to explain and to predict their magnetic properties, which are important for many practical applications.

3. Transition metal complexes

Unlike lanthanide complexes, *3d*-transition metal complexes are not so convenient for exploration by NMR spectroscopy for

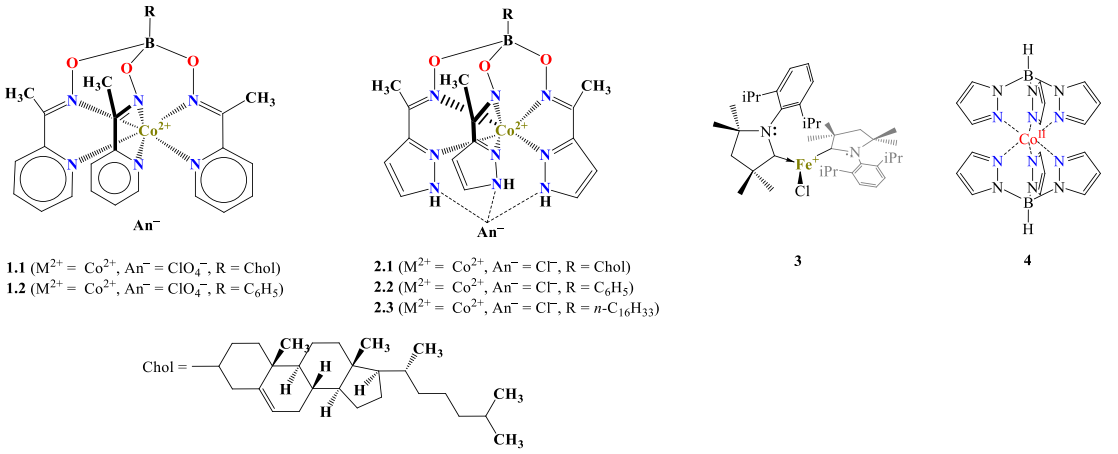

Scheme 3. *3d*-Transition metal complexes considered in the review.

a number of reasons. Firstly, the nuclear relaxation times of many transition metal ions are much shorter, which makes their spectra less resolved. Secondly, the periodicity of properties in lanthanide complexes allows one to reduce the number of unknown parameters in models that describe the experimental NMR data. In the case of *3d*-transition metals, some ions feature favorable characteristics for NMR, while some—not (Fig. 3). Thirdly, since the electronic properties of transition ions differ stronger, the complexes of various metals are seldom isostructural. Fourthly, an essential contribution of atomic *d*-orbitals of the metal ion to complex MOs implies significant delocalization of spin density, which leads to strong (in some cases even predominant) contact shifts; the calculation errors for the latter by quantum chemical methods are sometimes remarkable [52, 59–61]. All this leads to the scarce number of reports on NMR spectroscopic studies of paramagnetic transition metal complexes, which are mainly devoted to high-spin cobalt(II) complexes, appearing to be the most suitable compounds for NMR studies (Scheme 3).

In the case of low anisotropic ions (Cr^{III}, Mn^{II}, Cu^{II}, V^{IV}, *etc.*), for which the contact shifts predominate, the problem of the inaccuracy of their quantum chemical computation comes to the forefront [61]. At this moment, there is no method for the accurate definition of the electronic structures based on the NMR data for these ions [62].

However, in some cases, the application of conformationally rigid ligands allows one to overcome all the mentioned limitations. This can be illustrated by the analysis of NMR data for complexes **1.1** and **2.1** which refer to *tris*-oximate derivatives (clathrochelates) (Scheme 3) [64]. An interesting feature of these compounds is the presence of a conformationally rigid cage ligand, which structure remains unchanged in solution. Moreover, apical substituents in complexes **1.1** and **2.1** represent also conformationally rigid cholesterol moieties. Hence, many distant nuclei feature unchanged coordinates relative to the metal ion even in solution, and this distance provides the absence of contact shifts and the corresponding errors in quantum chemical calculations, *i.e.*, the nature of a paramagnetic shift for these nuclei is merely pseudocontact.

$$\delta_{par} = \frac{\Delta\chi_{ax}(3cos^2\theta-1)}{12\pi r^3} \qquad (15)$$

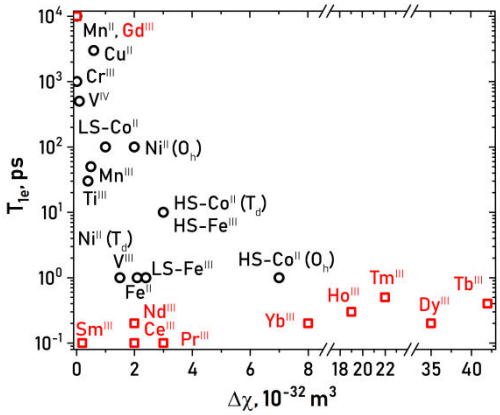

Figure 3. Typical values of electronic relaxation times (T_{1e}) and anisotropy of magnetic susceptibility tensor ($\Delta\chi$) for lanthanide (□) and transition metal ions (○). For the reference data, see Ref. [63].

Owing to such a specific molecular design, the convergence between the experimental and calculated shifts for these nuclei appeared to be close to the ideal one (Fig. 4, on the left) [61], which afforded the definition of the value of $\Delta\chi_{ax}$ with an unprecedented accuracy (0.013% for **1.1** and 0.118% for **2.1**). The convergence for the nuclei which do not refer to the conformationally rigid molecular moieties (protons of the CH_3-

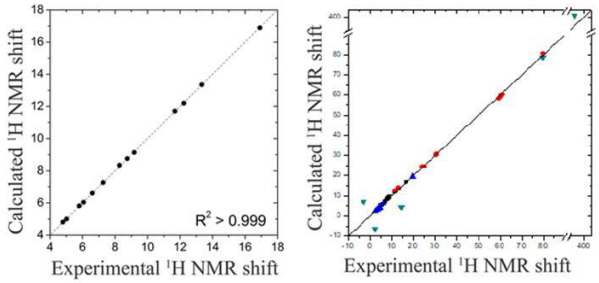

Figure 4. Convergence of the experimental and calculated chemical shifts. The left plot: for nuclei included in conformationally rigid molecular moieties and separated by more than 6 chemical bonds from the cobalt(II) ion. The right plot: for nuclei with significant contact contribution (●), with significant conformational dynamics (▲), included in the nearest surrounding of the metal ion (▼). (Reprinted with permission from A. A. Pavlov *et al.*, *ACS Omega*, **2018**, *3*, 4941–4946. DOI: 10.1021/acsomega.8b00772. Copyright (2018) American Chemical Society)

group, *etc*.) or featuring essential contact contribution is much worse (Fig. 4, on the right), which leads to the inaccurate definition of the values of $\Delta\chi_{ax}$.

Since clathrochelates appeared to be very suitable for paramagnetic NMR spectroscopy, this method was used for many of them and disclosed a number of interesting practical applications, such as spin switches [65], paramagnetic probes [66], and single-molecule magnets [67–70]. As it was already mentioned in the previous chapter, the knowledge of electronic structures is crucial for understanding the properties of these compounds as single-molecule magnets. In the case of transition metals, the model for description of an electronic structure of the ground state is somewhat simpler than for lanthanide analogs, since the spin–orbit interaction is not so high. As a rule, transition metal ions ($S > 1/2$) are described using the zero-field splitting formalism:

$$\hat{\boldsymbol{H}} = \mu_B \boldsymbol{g}\boldsymbol{B}\hat{\boldsymbol{S}} + D\left(\hat{\boldsymbol{S}}_{\boldsymbol{z}}^{\boldsymbol{2}} - \frac{1}{3}S(S+1)\right) + E\left(\hat{\boldsymbol{S}}_{\boldsymbol{x}}^{\boldsymbol{2}} - \hat{\boldsymbol{S}}_{\boldsymbol{y}}^{\boldsymbol{2}}\right) \quad (16)$$

where $\boldsymbol{g}$ is the g-tensor; ; $\hat{\boldsymbol{S}}$ and $\hat{\boldsymbol{S}}_{\boldsymbol{i}}$ are the operators of the electron momentum and its projection, respectively; D and E are the parameters of the tensor of zero-field splitting, which defines the electronic structure of the ground state in a zero magnetic field. From the viewpoint of SMM, the magnetization reversal barrier is proportional to the value of $|D|$ (17).

$$U = |D|S^2 \ (S = 1{,}2{,}3 \ldots) \quad (17a)$$

$$U = |D|(S^2 - 1/4) \ (S = \tfrac{3}{2}, \tfrac{5}{2}, \tfrac{7}{2} \ldots) \quad (17b)$$

Modeling of the values of $\Delta\chi_{ax}$, obtained based on the NMR data, by the Hamiltonian (16) provided the estimated values of D for a series of clathrochelates [66–70] and showed the potential of some of the complexes as SMM. Indeed, many of the explored complexes displayed high magnetization reversal barriers (Table 1) [71].

Table 1. Values of $2D$ for clathrochelates according to the data obtained by different methods

Compound	NMR	dc–Magnetometry	ac–Magnetometry	*ab initio*	Ref.
1.2	–190	–172	–195	–156	[69]
2.2	–218	–164	–152	–220	[67]
α-2.3	–174	–222	–192	–305	[68]
β-2.3	–174	–148	–109	–210	[68]

Many works considered above do not discuss the problem of structural differences in solution and in crystal; however, this problem is worth special consideration. A representative example is complex **2.3** which contains conformationally labile *n*-hexadecyl moiety (Scheme 3). In solution this complex exists in the form of various conformers which correspond to different conformations of each of $–CH_2–CH_2–$ fragments (*trans*, *gauche*+, or *gauche*–). The nucleus coordinates for different conformations can differ strongly, which, in turn, leads to different pseudocontact shifts (see (15)). On the other hand, it was shown that complex **2.3** can be crystallized as two polymorphs which differ in the conformation of $B–CH_2–CH_2–$ moiety (*trans* for α-polymorph and *gauche* for β-polymorph). It should be noted that the magnetic properties of these polymorphs differ significantly (Table 1). Since the energy barrier of a transition between *trans*, *gauche*+ or *gauche*– conformations seems to be not so high compared to kT, the NMR data are averaged by all conformations. Indeed the value of $2{\cdot}D$ according to the NMR data (174 cm^{-1}) is approximately equal to an average value between three conformers according to the data of dc-magnetometry (173 cm^{-1}).

It should be noted that most of the methods for the definition of a zero-field splitting (in particular, NMR spectroscopy) are indirect and the provided accuracy of estimation is low, which is evident from a comparison of the values obtained by different methods (Table 1). A prominent example of this divergence is iron(I) carbene complex **3**, which was explored in detail by different magnetic methods (Scheme 3). This complex is isoelectronic to cobalt(II) complexes (d^7-configuration) and, therefore, is a suitable object for investigation by NMR spectroscopy. The approximation of the magnetometric data in a constant field for complex **3** revealed the following magnetic parameters: $g_{iso} = 2.57$, $D = 20.4$ cm^{-1}, $E/D \approx 0$; the anisotropy of $\boldsymbol{g}$-tensor and rhomboidity of $\boldsymbol{D}$-tensor were not taken into account [72]. At the same time, according to the high-frequency EPR studies (336 GHz), the values of $\boldsymbol{g}$-tensor appeared to be different ($g_x = 3.34$, $g_y = 3.32$, $g_z = 2.91$) at the same value of $\boldsymbol{D}$ [72]. It is noteworthy that the isotropic value of g_{iso}, obtained by magnetometry, is lower than any value of the component (g_x, g_y, g_z) derived from EPR, *i.e.*, the data of these two methods were not described by the same set of parameters. The exploration of complex **3** in solution by NMR spectroscopy [59] showed slow dynamics of the C(Fe)–N–C–C torsion angle (Scheme 3), which led to an extremely low resolution at room temperature. Nevertheless, at 233.2 K the dynamic processes slowed down and the values of $\Delta\chi_{ax}$ and $\Delta\chi_{rh}$ were defined [59]. The value of the energy of a zero-field splitting calculated using these data (D = 55.8 cm^{-1}, E/D = 0.15) strongly differs from that obtained from magnetometric studies and EPR in solid state (*vide supra*), which can result both from different structures in solution and in crystal and the problem of overparametrization stated by Ishikawa [25], which is not discussed by the authors of these works.

As well as in the case of lanthanide complexes, the application of a combination of methods, which data are described within one model, can give more accurate and detailed information about the electronic structures [25]; however, for transition ions these works are very scarce. One of the transition metal complexes extensively studied by magnetic methods is cobalt(II) *tris*-pyrazolylborate **4** (Scheme 3). The detailed analysis of the EPR spectra (X- and Q-range) of complex **4** along with the data of optical spectroscopy was made over 50 years ago [73]. It was shown that the value of spin–orbit interaction in complex **4** is too high and becomes comparable to the energy of crystal field splitting. In this case the model of zero-field splitting (16) is inapplicable, and the spin–orbit interaction must be considered in an explicit form:

$$\hat{\boldsymbol{H}}_{SOC} = \sigma\lambda\hat{\boldsymbol{L}} \cdot \hat{\boldsymbol{S}} \quad (18)$$

where λ is the constant of a spin–orbit interaction, σ is the attenuation coefficient, and $\hat{\mathrm{L}}$ and $\hat{\boldsymbol{S}}$ are the operators of orbital and spin momentum, respectively. The application of model (18) led to the more complex electronic structure (Fig. 5), in which each KD corresponds to a combination of spin and orbital magnetic quantum numbers (m_l = –1, 0, +1; m_s = –3/2, –1/2, +1/2, +3/2).

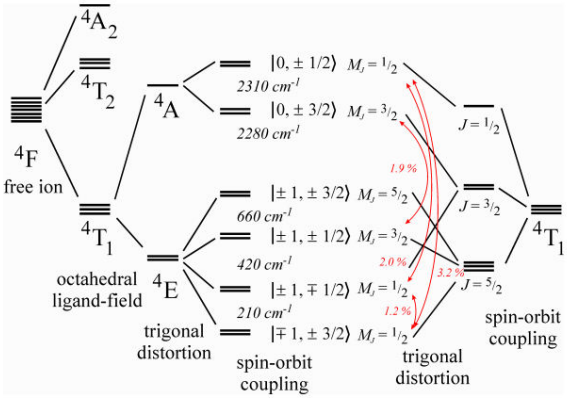

Figure 5. Electronic structure of complex **4** according to the data of EPR and optical spectroscopy. (Reproduced with permission from J. Jesson, J. Chem. Phys. 45, 1049 (1966). Copyright 1966, AIP Publishing)

Subsequently, the analysis of the NMR data along with the terahertz EPR data and the data on magnetic susceptibility in solution (the Evans method) confirmed the earlier suggested electronic structure [74]. It was shown that a broad set of the experimental data obtained by these three methods can solve the problem of overparametrization, since the zero-field splitting model (16) appeared to be unsupported for simultaneous description of these data. Only upon application of the unique Hamiltonian parameters (19), which take into account the spin–orbit interaction in an explicit form [75], one can obtain the correct description of the experimental data; any deviation of the parameters from the optimal ones leads to deterioration of the data convergence at least by one of the methods [74].

$$\widehat{\mathcal{H}} = \sigma\lambda\hat{\boldsymbol{L}}\cdot\hat{\boldsymbol{S}} + \Delta\left(3\hat{\boldsymbol{L}}_z^2 - \hat{\boldsymbol{L}}^2\right) + \mu_B B_0\left(-\sigma\hat{\boldsymbol{L}} + g_e\hat{\boldsymbol{S}}\right) \quad (19)$$

The electronic structure assigned by this method is in full agreement with the data obtained earlier by other methods (ENDOR EPR spectroscopy [76, 77] and magnetometry [78]). The example of complex **4** shows that the description model during the analysis of magnetic data should be carefully chosen, although in most cases the zero-field splitting formalism is used for transition metal complexes. In the case of compound **4**, the data of THz-EPR and the Evans method can be satisfactorily described by this formalism, but the introduction of the NMR data reveals the inadequacy of the zero-field splitting model.

4. Conclusions

In this review, we showed that NMR spectroscopy is a reliable and important source of information about the electronic structures of paramagnetic lanthanide and transition metal complexes. In the absence of the NMR data, the classical magnetic methods (magnetometry and EPR) often face the problem of overparametrization of the model which describes the electronic structure. The peculiarities and problems of the application of NMR spectroscopy in practice are considered, the main issues are the following ones. (1) Since NMR studies are carried out in solution, it is necessary to take into account different dynamic processes (conformational dynamics, chemical exchange, and so on) because they strongly affect the values of paramagnetic shifts. (2) The problem of evaluation of a contact shift in the case of low anisotropic ions (Mn^{II}, Cu^{II}, and Cr^{III}) makes NMR a low-effective method, but for the ions with high magnetic anisotropy, especially lanthanide(III) ions (expect for Gd^{III}), this is not crucial. (3) The lanthanide ions are more preferred for paramagnetic NMR than *3d*-metal ions, since the properties of isostructural complexes of different ions regularly depend on the number of unpaired electrons, which simplifies the analysis of the resulting data. (4) The model for description of the NMR data should be chosen carefully. In particular, during the description of lanthanide ions, Bleaney's theory is often used, while in the case of *3d*-metal ions—the zero-field splitting formalism. However, the current review showed that there are many exceptions to this rule.

Acknowledgements

This work was supported by the Russian Science Foundation, project no. 18-73-00113.

Corresponding author

* E-mail: pavlov@ineos.ac.ru. (A. A. Pavlov)

References

1. G. Molnár, S. Rat, L. Salmon, W. Nicolazzi, A. Bousseksou, *Adv. Mater.*, **2018**, *30*, 1703862. DOI: 10.1002/adma.201703862
2. D. N. Woodruff, R. E. P. Winpenny, R. A. Layfield, *Chem. Rev.*, **2013**, *113*, 5110–5148. DOI: 10.1021/cr400018q
3. J. M. Frost, K. L. M. Harriman, M. Murugesu, *Chem. Sci.*, **2016**, *7*, 2470–2491. DOI: 10.1039/C5SC03224E
4. L. Bogani, W. Wernsdorfer, *Nanosci. Technol.*, **2009**, 194–201. DOI: 10.1142/9789814287005_0020
5. Available from: webofknowledge.com
6. E. Ravera, G. Parigi, C. Luchinat, *J. Magn. Reson.*, **2019**, *306*, 173–179. DOI: 10.1016/j.jmr.2019.07.027
7. E. Ravera, G. Parigi, C. Luchinat, *J. Magn. Reson.*, **2017**, *282*, 154–169. DOI: 10.1016/j.jmr.2017.07.013
8. C. Nitsche, G. Otting, *Prog. Nucl. Magn. Reson. Spectrosc.*, **2017**, *98*, 20–49. DOI: 10.1016/j.pnmrs.2016.11.001
9. T. Müntener, J. Kottelat, A. Huber, D. Häussinger, *Bioconjugate Chem.*, **2018**, *29*, 3344–3351. DOI: 10.1021/acs.bioconjchem.8b00512
10. O. A. Blackburn, R. M. Edkins, S. Faulkner, A. M. Kenwright, D. Parker, N. J. Rogers, S. Shuvaev, *Dalton Trans.*, **2016**, *45*, 6782–6800. DOI: 10.1039/C6DT00227G
11. G. Parigi, L. Benda, E. Ravera, M. Romanelli, C. Luchinat, *J. Chem. Phys.*, **2019**, *150*, 144101. DOI: 10.1063/1.5037428
12. L. Benda, J. Mareš, E. Ravera, G. Parigi, C. Luchinat, M. Kaupp, J. Vaara, *Angew. Chem., Int. Ed.*, **2016**, *55*, 14713–14717. DOI: 10.1002/anie.201608829
13. A. C. Harnden, D. Parker, N. J. Rogers, *Coord. Chem. Rev.*, **2019**, *383*, 30–42. DOI: 10.1016/j.ccr.2018.12.012
14. P. K. Senanayake, N. J. Rogers, K.-L. N. A. Finney, P. Harvey, A. M. Funk, J. I. Wilson, D. O'Hogain, R. Maxwell, D. Parker, A. M. Blamire, *Magn. Reson. Med.*, **2017**, *77*, 1307–1317. DOI: 10.1002/mrm.26185
15. Y. Rechkemmer, J. E. Fischer, R. Marx, M. Dörfel, P. Neugebauer, S. Horvath, M. Gysler, T. Brock-Nannestad, W. Frey, M. F. Reid, J. van Slageren, *J. Am. Chem. Soc.*, **2015**, *137*, 13114–13120. DOI: 10.1021/jacs.5b08344
16. L. Ungur, L. F. Chibotaru, *Chem. Eur. J.*, **2017**, *23*, 3708–3718. DOI: 10.1002/chem.201605102

17. G. Cucinotta, M. Perfetti, J. Luzon, M. Etienne, P.-E. Car, A. Caneschi, G. Calvez, K. Bernot, R. Sessoli, *Angew. Chem.*, *Int. Ed.*, **2012**, *51*, 1606–1610. DOI: 10.1002/anie.201107453
18. B. M. Flanagan, P. V. Bernhardt, E. R. Krausz, S. R. Lüthi, M. J. Riley, *Inorg. Chem.*, **2002**, *41*, 5024–5033. DOI: 10.1021/ic011276q
19. B. M. Flanagan, P. V. Bernhardt, E. R. Krausz, S. R. Lüthi, M. J. Riley, *Inorg. Chem.*, **2001**, *40*, 5401–5407. DOI: 10.1021/ic0103244
20. N. Ishikawa, M. Sugita, T. Okubo, N. Tanaka, T. Iino, Y. Kaizu, *Inorg. Chem.*, **2003**, *42*, 2440–2446. DOI: 10.1021/ic026295u
21. N. Ishikawa, M. Sugita, T. Ishikawa, S.-y. Koshihara, Y. Kaizu, *J. Am. Chem. Soc.*, **2003**, *125*, 8694–8695. DOI: 10.1021/ja029629n
22. N. Ishikawa, *Polyhedron*, **2007**, *26*, 2147–2153. DOI: 10.1016/j.poly.2006.10.022
23. K. W. H. Stevens, *Proc. Phys. Soc.*, *Sect. A*, **1952**, *65*, 209–215. DOI: 10.1088/0370-1298/65/3/308
24. A. Abragam, B. Bleaney, *Electron Paramagnetic Resonance*, Oxford, Clarendon, **1970**.
25. N. Ishikawa, *J. Phys. Chem. A*, **2003**, *107*, 5831–5835. DOI: 10.1021/jp034433a
26. E. A. Suturina, J. Nehrkorn, J. M. Zadrozny, J. Liu, M. Atanasov, T. Weyhermüller, D. Maganas, S. Hill, A. Schnegg, E. Bill, *Inorg. Chem.*, **2017**, *56*, 3102–3118. DOI: 10.1021/acs.inorgchem.7b00097
27. M. Vonci, K. Mason, E. A. Suturina, A. T. Frawley, S. G. Worswick, I. Kuprov, D. Parker, E. J. McInnes, N. F. Chilton, *J. Am. Chem. Soc.*, **2017**, *139*, 14166–14172. DOI: 10.1021/jacs.7b07094
28. A. J. Pell, G. Pintacuda, C. P. Grey, *Prog. Nucl. Magn. Reson. Spectrosc.*, **2019**, *111*, 1–271. DOI: 10.1016/j.pnmrs.2018.05.001
29. B. Bleaney, *J. Magn. Reson.*, **1972**, *8*, 91–100. DOI: 10.1016/0022-2364(72)90027-3
30. D. P. Arnold, J. Jiang, *J. Phys. Chem. A*, **2001**, *105*, 7525–7533. DOI: 10.1021/jp0105847
31. M. Hiller, M. Maier, H. Wadepohl, M. Enders, *Organometallics*, **2016**, *35*, 1916–1922. DOI: 10.1021/acs.organomet.6b00241
32. J. Van Vleck, *The Theory of Electric and Magnetic Susceptibilities*, Oxford, Clarendon, **1932**.
33. N. Ishikawa, M. Sugita, T. Ishikawa, S.-y. Koshihara, Y. Kaizu, *J. Phys. Chem. B*, **2004**, *108*, 11265–11271. DOI: 10.1021/jp0376065
34. H. Wang, K. Qian, K. Wang, Y. Bian, J. Jiang, S. Gao, *Chem. Commun.*, **2011**, *47*, 9624–9626. DOI: 10.1039/c1cc12509e
35. H. Wang, T. Liu, K. Wang, C. Duan, J. Jiang, *Chem. Eur. J.*, **2012**, *18*, 7691–7694. DOI: 10.1002/chem.201200552
36. H. Wang, B.-W. Wang, Y. Bian, S. Gao, J. Jiang, *Coord. Chem. Rev.*, **2016**, *306*, 195–216. DOI: 10.1016/j.ccr.2015.07.004
37. N. Ishikawa, T. Iino, Y. Kaizu, *J. Phys. Chem. A*, **2002**, *106*, 9543–9550. DOI: 10.1021/jp0209244
38. N. Ishikawa, T. Iino, Y. Kaizu, *J. Am. Chem. Soc.*, **2002**, *124*, 11440–11447. DOI: 10.1021/ja027119n
39. N. Ishikawa, S. Otsuka, Y. Kaizu, *Angew. Chem.*, *Int. Ed.*, **2005**, *44*, 731–733. DOI: 10.1002/anie.200461546
40. D. Tanaka, T. Inose, H. Tanaka, S. Lee, N. Ishikawa, T. Ogawa, *Chem. Commun.*, **2012**, *48*, 7796–7798. DOI: 10.1039/c2cc00086e
41. T. Inose, D. Tanaka, H. Tanaka, O. Ivasenko, T. Nagata, Y. Ohta, S. De Feyter, N. Ishikawa, T. Ogawa, *Chem. Eur. J.*, **2014**, *20*, 11362–11369. DOI: 10.1002/chem.201402669
42. A. Santria, A. Fuyuhiro, T. Fukuda, N. Ishikawa, *Dalton Trans.*, **2019**, *48*, 7685–7692. DOI: 10.1039/C9DT00915A
43. F. Gao, M.-X. Yao, Y.-Y. Li, Y.-Z. Li, Y. Song, J.-L. Zuo, *Inorg. Chem.*, **2013**, *52*, 6407–6416. DOI: 10.1021/ic400245n
44. P. Comba, M. Enders, M. Großhauser, M. Hiller, D. Müller, H. Wadepohl, *Dalton Trans.*, **2017**, *46*, 138–149. DOI: 10.1039/C6DT03488H
45. E. A. Suturina, K. Mason, M. Botta, F. Carinato, I. Kuprov, N. F. Chilton, E. J. L. McInnes, M. Vonci, D. Parker, *Dalton Trans.*, **2019**, *48*, 8400–8409. DOI: 10.1039/C9DT01069F
46. M. Hiller, S. Krieg, N. Ishikawa, M. Enders, *Inorg. Chem.*, **2017**, *56*, 15285–15294. DOI: 10.1021/acs.inorgchem.7b02704
47. J. A. Peters, J. Huskens, D. J. Raber, *Prog. Nucl. Magn. Reson. Spectrosc.*, **1996**, *28*, 283–350. DOI: 10.1016/0079-6565(95)01026-2
48. A. Bax, J. J. Chou, B. E. Ramirez, *eMagRes*, **2007**. DOI: 10.1002/9780470034590.emrstm0262
49. C. N. Reilley, B. W. Good, R. D. Allendoerfer, *Anal. Chem.*, **1976**, *48*, 1446–1458. DOI: 10.1021/ac50005a010
50. A. A. Pinkerton, M. Rossier, S. Spiliadis, *J. Magn. Reson.*, **1985**, *64*, 420–425. DOI: 10.1016/0022-2364(85)90104-0
51. G. Castro, M. Regueiro-Figueroa, D. Esteban-Gómez, P. Pérez-Lourido, C. Platas-Iglesias, L. Valencia, *Inorg. Chem.*, **2016**, *55*, 3490–3497. DOI: 10.1021/acs.inorgchem.5b02918
52. M. Damjanovic, K. Katoh, M. Yamashita, M. Enders, *J. Am. Chem. Soc.*, **2013**, *135*, 14349–14358. DOI: 10.1021/ja4069485
53. F. Gendron, B. Pritchard, H. Bolvin, J. Autschbach, *Dalton Trans.*, **2015**, *44*, 19886–19900. DOI: 10.1039/C5DT02858B
54. L. Ungur, J. J. Le Roy, I. Korobkov, M. Murugesu, L. F. Chibotaru, *Angew. Chem.*, *Int. Ed.*, **2014**, *53*, 4413–4417. DOI: 10.1002/anie.201310451
55. J. D. Rinehart, J. R. Long, *Chem. Sci.*, **2011**, *2*, 2078–2085. DOI: 10.1039/c1sc00513h
56. K. L. M. Harriman, I. Korobkov, M. Murugesu, *Organometallics*, **2017**, *36*, 4515–4518. DOI: 10.1021/acs.organomet.7b00449
57. M. Hiller, T. Sittel, H. Wadepohl, M. Enders, *Chem. Eur. J.*, **2019**, *25*, 10668–10677. DOI: 10.1002/chem.201901388
58. V. S. Mironov, Y. G. Galyametdinov, A. Ceulemans, C. Görller-Walrand, K. Binnemans, *J. Chem. Phys.*, **2002**, *116*, 4673–4685. DOI: 10.1063/1.1450543
59. M. Damjanović, P. P. Samuel, H. W. Roesky, M. Enders, *Dalton Trans.*, **2017**, *46*, 5159–5169. DOI: 10.1039/C7DT00408G
60. M. Kruck, H. Wadepohl, M. Enders, L. H. Gade, *Chem. Eur. J.*, **2013**, *19*, 1599–1606. DOI: 10.1002/chem.201203450
61. A. A. Pavlov, S. A. Savkina, A. S. Belov, Y. Z. Voloshin, Y. V. Nelyubina, V. V. Novikov, *ACS Omega*, **2018**, *3*, 4941–4946. DOI: 10.1021/acsomega.8b00772
62. J. Krzystek, G. Kohl, H.-B. Hansen, M. Enders, J. Telser, *Organometallics*, **2019**, *38*, 2179–2188. DOI: 10.1021/acs.organomet.9b00158
63. I. Bertini, C. Luchinat, G. Parigi, E. Ravera, *NMR of Paramagnetic Molecules: Applications to Metallobiomolecules and Models*, vol. 2, Amsterdam, Elsevier, **2016.**
64. Y. Voloshin, I. Belaya, R. Krämer, *Cage Metal Complexes: Clathrochelates Revisited*, Springer, Cham, **2017**.
65. V. V. Novikov, I. V. Ananyev, A. A. Pavlov, M. V. Fedin, K. A. Lyssenko, Y. Z. Voloshin, *J. Phys. Chem. Lett.*, **2014**, *5*, 496–500. DOI: 10.1021/jz402678q
66. V. V. Novikov, A. A. Pavlov, A. S. Belov, A. V. Vologzhanina, A. Savitsky, Y. Z. Voloshin, *J. Phys. Chem. Lett.*, **2014**, *5*, 3799–3803. DOI: 10.1021/jz502011z
67. V. V. Novikov, A. A. Pavlov, Y. V. Nelyubina, M.-E. Boulon, O. A. Varzatskii, Y. Z. Voloshin, R. E. Winpenny, *J. Am. Chem. Soc.*, **2015**, *137*, 9792–9795. DOI: 10.1021/jacs.5b05739
68. A. A. Pavlov, Y. V. Nelyubina, S. V. Kats, L. V. Penkova, N. N. Efimov, A. O. Dmitrienko, A. V. Vologzhanina, A. S. Belov, Y. Z. Voloshin, V. V. Novikov, *J. Phys. Chem. Lett.*, **2016**, *7*, 4111–4116. DOI: 10.1021/acs.jpclett.6b02091
69. A. A. Pavlov, S. A. Savkina, A. S. Belov, Y. V. Nelyubina, N. N. Efimov, Y. Z. Voloshin, V. V. Novikov, *Inorg. Chem.*, **2017**, *56*, 6943–6951. DOI: 10.1021/acs.inorgchem.7b00447
70. A. A. Pavlov, D. Y. Aleshin, S. A. Savkina, A. S. Belov, N. N. Efimov, J. Nehrkorn, M. Ozerov, Y. Z. Voloshin, Y. V. Nelyubina, V. V. Novikov, *ChemPhysChem*, **2019**, *20*, 1001–1005. DOI: 10.1002/cphc.201900219

71. V. V. Novikov, Molecular Magnetism of Cobalt Cage Complexes, *Doctoral (Chem.) Dissertation*, Moscow, INEOS RAS, **2018**, p. 285.
72. P. P. Samuel, K. C. Mondal, N. Amin Sk, H. W. Roesky, E. Carl, R. Neufeld, D. Stalke, S. Demeshko, F. Meyer, L. Ungur, L. F. Chibotaru, J. Christian, V. Ramachandran, J. van Tol, N. S. Dalal, *J. Am. Chem. Soc.*, **2014**, *136*, 11964–11971. DOI: 10.1021/ja5043116
73. J. Jesson, *J. Chem. Phys.*, **1966**, *45*, 1049–1056. DOI: 10.1063/1.1727656
74. A. A. Pavlov, J. Nehrkorn, Y. A. Pankratova, M. Ozerov, E. A. Mikhalyova, A. V. Polezhaev, Y. V. Nelyubina, V. V. Novikov, *Phys. Chem. Chem. Phys.*, **2019**, *21*, 8201–8204. DOI: 10.1039/C9CP01474H
75. M. A. Palacios, J. Nehrkorn, E. A. Suturina, E. Ruiz, S. Gómez-Coca, K. Holldack, A. Schnegg, J. Krzystek, J. M. Moreno, E. Colacio, *Chem. Eur. J.*, **2017**, *23*, 11649–11661. DOI: 10.1002/chem.201702099
76. W. K. Myers, C. P. Scholes, D. L. Tierney, *J. Am. Chem. Soc.*, **2009**, *131*, 10421–10429. DOI: 10.1021/ja900866y
77. W. K. Myers, E. N. Duesler, D. L. Tierney, *Inorg. Chem.*, **2008**, *47*, 6701–6710. DOI: 10.1021/ic800245k
78. J. Zhang, J. Li, L. Yang, C. Yuan, Y.-Q. Zhang, Y. Song, *Inorg. Chem.*, **2018**, *57*, 3903–3912. DOI: 10.1021/acs.inorgchem.8b00055

Translated by D. V. Aleksanyan